# JQS

## **Journal of Quaternary Science**



# Late Pleistocene to Holocene paleoenvironmental changes in the NW Black Sea

ANDREI BRICEAG,  $^{1*}$  ANASTASIA YANCHILINA,  $^{2}$  WILLIAM B. F. RYAN,  $^{2}$  MARIUS STOICA  $^{3}$  and MIHAELA C. MELINTE-DOBRINESCU  $^{1}$ 

<sup>1</sup>National Institute of Marine Geology and Geo-Ecology, GeoEcoMar, Bucharest, Romania

Received 7 July 2017; Revised 24 October 2018; Accepted 6 December 2018

ABSTRACT: Two gravity cores that penetrated Upper Pleistocene to Upper Holocene sediments in the NW Black Sea have been studied lithologically and microfaunally. The investigations have been coupled with isotopic, calcium carbonate and radiocarbon dating. Six ecological intervals have been distinguished based on changes in microfossil assemblages, giving new insights on the sea-level and paleoenvironmental changes that took place in the last 25 000 a BP. For the Last Glacial Maximum the ostracod community contains a homogeneous brackish assemblage dominated by Candonidae, suggesting a salinity around 5–8%. The salinity decrease (to 0.5–5%) that started concomitantly with the first Meltwater Pulse during Heinrich Stadial 1 is mirrored by increasing diversity and abundance of microfaunal assemblages. This microfaunal increase reached maximum values within the Bølling–Allerød warm period. The shift from Loxoconchidae to Candonidae towards the top of the Younger Dryas suggests a slight increase in salinity. The Preboreal warming period is marked by an abundance increase of ostracod assemblages. During the Late Holocene, stable marine conditions set in, reflected by assemblages similar to those of the present-day. Based on these data, the first marine influx into the Black Sea before 9390 a BP is assumed. © 2019 John Wiley & Sons, Ltd.

KEYWORDS: foraminifers; ostracods; radiocarbon dating; Romanian Black Sea shelf; stable isotopes.

### Introduction

The Black Sea basin opened during the Late Cretaceous, as a back-arc extensional basin associated with subduction of the Paleo-Tethys and Neo-Tethys Oceans (Letouzey et al., 1977; Nikishin et al., 2001; Dinu et al., 2005). During global ocean low-stands, the Black Sea basin evolved as a giant water body isolated from the Mediterranean. Since the last deglaciation, the Black Sea and Mediterranean were connected via the Marmara Sea through the narrow Bosphorus and Dardanelles Straits (Ross and Degens, 1974; Chepalyga, 1984; Aksu et al., 2002). Several scenarios were advanced regarding the reconnection between the Mediterranean and Black Sea. Ryan et al. (1997) proposed a catastrophic flood that took place at a rate approaching tens of cm per day sea-level rise. They assumed that the Mediterranean sea-level had risen significantly; hence, the waters invaded the isolated Black Sea basin in a cascade at  $\sim$  7150 a BP. Another hypothesis (Aksu et al., 1999, 2002; Hiscott et al., 2002, 2007; Kaminski et al., 2002) assumed that there was no rapid entry of salt water during reconnection between the two marine basins. Therefore, at  $\sim 11\,900$  a BP, there was an outflow of Black Sea waters through the Bosphorus Strait in the Mediterranean, while between  $\sim 8500$  and 8000 a BP the two-way water circulation between the Black Sea and the Mediterranean was established through the Bosphorus Strait (Marret et al., 2009). Based on the pattern of fluctuation of foraminiferal assemblages from the Black Sea, Yanko-Hombach (2007) proposed a oscillatory reconnection. This scenario allowed successive waves of Mediterranean immigrants to enter the Black Sea basin during six transgression-regression stages. Yanko-Hombach suggested that the first connection between

the Black Sea and Mediterranean may not have been through the Bosphorus Strait, but through alternative routes, such as Izmit Bay – Sapanca Lake – Sakarya River.

In the Late Pleistocene – Holocene interval, the water level of the Black Sea was controlled by regional rather than global climatic modifications (Lericolais et al., 2010). During the Last Glacial Maximum (LGM), i.e. ~ 25 000-18 000 a BP, the water level of the Black Sea was at least 100 m lower than today and the basin had a freshwater character (Fedorov, 1972; Yanko, 1990; Ryan et al., 1997; Popescu et al., 2001; Oaie and Melinte-Dobrinescu, 2012; Lericolais et al., 2013). According to Major et al. (2002, 2006) and Bahr et al. (2005), the LGM interval was characterized by stable climatic conditions. Wegwerth et al. (2016) studied in detail the last glacial stage of the Black Sea and reconstructed the riverine and eolian input, salinity and productivity in the SE Black Sea. They show that riverine nutrient supply and basin surface productivity were relatively low during the stadials, while bottom waters were well oxygenated, favoring the occurrence of benthic ostracods.

After this period, during Heinrich Stadial 1 (HS-1, ~18 000–14 700 cal a BP), the first Fennoscandian Meltwater Pulse in the Black Sea occurred, which recorded a high deglacial sediment load represented by reddish-brown clays (Major *et al.*, 2002; Ryan *et al.*, 2003; Bahr *et al.*, 2005; Soulet *et al.*, 2011a, 2013; Constantinescu *et al.*, 2015). It has been suggested that, during this period, Caspian Sea spillover into the Black Sea occurred through the Manych Depression (Fig. 1) due to the meltwater delivered to the Volga and low evaporation rates resulting from low temperatures (Chepalyga, 1984; Chepalyga *et al.*, 2004; Bahr *et al.*, 2005; Major *et al.*, 2006). This Caspian overflow has been attributed to the Early Khvalynian transgression, caused by pulses of meltwater from the Fennoscandia and/or Barents–Kara ice sheets

\*Correspondence: Andrei Briceag, as above E-mail: andrei.briceag@geoecomar.ro

<sup>&</sup>lt;sup>2</sup>Lamont-Doherty Earth Observatory of Columbia University, Palisades, NY, USA

<sup>&</sup>lt;sup>3</sup>Faculty of Geology and Geophysics, University of Bucharest, Bucharest, Romania

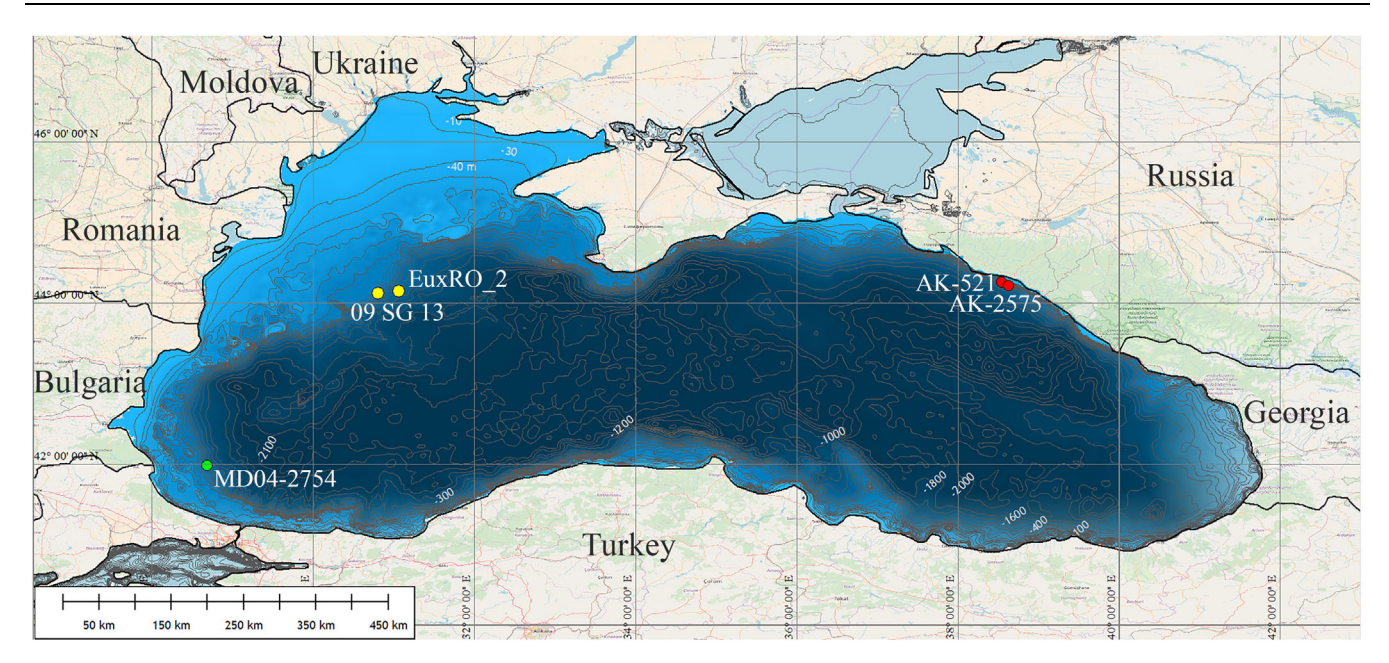


**Figure 1.** Location of the studied cores (yellow circles), core MD04\_2754 (green circle) studied by Boomer *et al.* (2010) and cores AK-521 and AK-2575 (red circles) studied by Ivanova *et al.* (2007, 2015) and Zenina *et al.* (2017). Map source: Open Street Map.

(Grosswald, 1980; Kroonenberg *et al.*, 1997; Grosswald and Hughes, 2002; Ryan, 2007). During this transgression, the Caspian Sea accumulated its characteristic 'chocolate clays' that resemble the color of the brown–red clay observed in the Black Sea cores (Ryan, 2007).

Recent studies on the presence of similar red clays (Soulet et al., 2013) linked their origin to two possible provenances: (i) drainage of the Fennoscandian ice sheet through the Dnieper River, via proglacial Lake Disna into the Black Sea, or (ii) through the Danube River, supplied by glaciers from the Alps (Fig. 1). Ryan (2007) identified in several cores four distinct intervals of brown-red clay, interbedded with gray clays. Bahr et al. (2005) identified in the NW Black Sea (south of the Danube Delta), four major flooding intervals, each lasting hundreds of years. These authors hypothesize that each layer, with millimeter-scale laminations, might correspond to annual pulses of meltwater discharge. Ryan et al. (2013) summarized data from more than 30 cores from the western Black Sea and indicate the presence of red clays in all of them. They observed that these red clays do not occur in the eastern Black Sea,.

Based on the elemental geochemistry of Upper Pleistocene and Holocene sediments of the Black Sea, Piper and Calvert (2011) identified two terrigenous sources: one includes Anatolia and the southern Caucasus, and another represents rivers entering the Black Sea from Eastern Europe. The authors show that the relative contribution of the two sources shifted abruptly every few thousand years during the Lateglacial and Early Holocene lacustrine phase of the basin.

Soulet *et al.* (2011a, 2013), based on reservoir age reconstructions, suggest that, at the end of the Black Sea Meltwater Pulses, water level was  $-30\,\text{m}$  below the present-day level. This event is associated with the Bølling–Allerød warm period Black Sea highstand (Lericolais *et al.*, 2010). Following the Younger Dryas cold period, a new water level down to  $-100\,\text{m}$  occurred (Lericolais *et al.*, 2010).

The hydrological evolution of the Black Sea is well reflected in ostracod assemblages. Numerous microfaunal studies providing new insights into past environmental conditions during the Late Pleistocene–Holocene have been published (Hiscott *et al.*, 2007; Ivanova *et al.*, 2007, 2012, 2015; Yanko-Hombach, 2007; Opreanu, 2008;

Boomer et al., 2010; Briceag et al., 2012, 2014, 2016; Zenina et al., 2017). Zenina et al. (2017) identified at ~9600 a BP the first Mediterranean ostracod immigrants. Ivanova et al. (2015) reported between 8800 and 6700 a BP a mixed Caspian and Mediterranean ostracod assemblage that points to sustained co-habitation, reflecting a gradual increase in bottom water salinity from 7 to 18‰. From 6800 a BP the ostracod faunas become dominated by Mediterranean taxa (Zenina et al., 2017).

The aim of this study is to refine the Romanian Black Sea shelf stratigraphy for the last 25 000 a BP, to decipher the paleoenvironmental and paleoecological conditions based on integration of the fossil record (i.e. micro- and macrofaunas) with the oxygen isotope fluctuations, CaCO<sub>3</sub> values and accelerator mass spectrometry (AMS) <sup>14</sup>C dating. Detailed micropaleontological studies, based on ostracod and foraminiferal analyses, are discussed herein.

### Regional setting

Today, the Black Sea is the largest marine anoxic basin in the world (Georgiev, 1967; Chepalyga, 1984). Its anoxic character is given by a stable pycnocline at around 200 m water depth that separates the deep anoxic and more saline waters (around 23‰) containing a high hydrogen sulphide concentration from the less saline (around 17–18‰), and oxygenated surface waters (Chepalyga, 1984; Özsoy *et al.*, 1995; Bahr *et al.*, 2006; Piper and Calvert, 2009). This vertical stratification is given by two strong directional currents that exist through the Bosphorus Strait: a deep water current of high-salinity Mediterranean water that enters the Black Sea basin and a surface outflow current, which expels low-salinity waters into the Marmara Sea (Gunnerson and Ozturgut, 1974; Major *et al.*, 2002).

The NW Black Sea continental shelf covers almost 30% of the total Black Sea basin and 94% of the total shelf geomorphologic province (Goncharov, 1958). The Danube, Dniester, Dnieper and Southern Bug rivers provide important fluvial water and sediment discharge into this area (Tolmazin, 1985; Margvelashvily *et al.*, 1999; Hiscott *et al.*, 2007). Nevertheless, the main source of water and sediment to the NW Black Sea shelf is the Danube; the Dniester, Dnieper and

Southern Bug discharge most of their sediments today into isolated lagoons and limans, separated by sand barriers from the open basin (Balkas *et al.*, 1990; Panin and Jipa, 2002).

In the deep parts of the basin, below 200 m, three sedimentary successions characterize the Holocene deposits (Ross and Degens, 1974): the oldest Unit 3 (Lacustrine Lutite) is Late Pleistocene – Early Holocene in age; Unit 2 (Sapropelic Mud), covering the Early to Middle Holocene interval, corresponds to the establishment of anoxic conditions in the basin; and the youngest Unit 1 (Coccolithic Mud), Middle Holocene to Recent, consists of microlaminated coccolith ooze.

### Material and methods

### Study sites

In this study, two Kullenberg gravity cores, 09 SG 13 (44° 07′12.24″N, 30°48′5.22″E; 200 m water depth; 396 cm long; Figs 1 and 2) and EuxRO\_2 (44°8′53.99″N, 31°4′0.30″E; 500 m water depth; 432 cm long; Figs 1 and 2), collected from the NW Black Sea shelf were analyzed. In core EuxRO\_2, only the uppermost 70 cm was investigated, to complete the litho- and biostratigraphy. Preliminary studies on 09 SG 13 core were presented by Briceag *et al.* (2016).

### Microfossil analysis

In all, 120 samples were processed for microfossil analyses by boiling with  $Na_2CO_3$  and washing through a 63- $\mu m$  sieve (100 samples from core 09 SG 13 and 20 from core EuxRO\_02). Both scanning electron microscopy (SEM) and stereomicroscope investigations were performed. Ostracod and foraminiferal assemblages were investigated for diversity and abundance. For ostracods, the adult, the juvenile and the carapaces were considered separately. This method allows the differentiation between in situ and transported taxa (Boomer et al., 2003). For quantitative analyses of ostracods, we have considered only adult specimens (whole adult specimens of each sample were counted). Due to the possibility of successive molt of taxa, juvenile specimens were not taken into account. For the core 09 SG 13, the most abundant sample contains 46 specimens, the least abundant sample three specimens and the mean value for all the samples is 15.3 specimens. For core EuxRO 2, the most abundant sample contains 355 specimens, the least abundant sample is barren and the mean value for all the samples is 85.9 specimens.

Based on the fluctuation of the microfossil assemblages in abundance and diversity, ecological intervals have been defined. The ecological affinities of each species, such as salinity and temperature, were also considered.

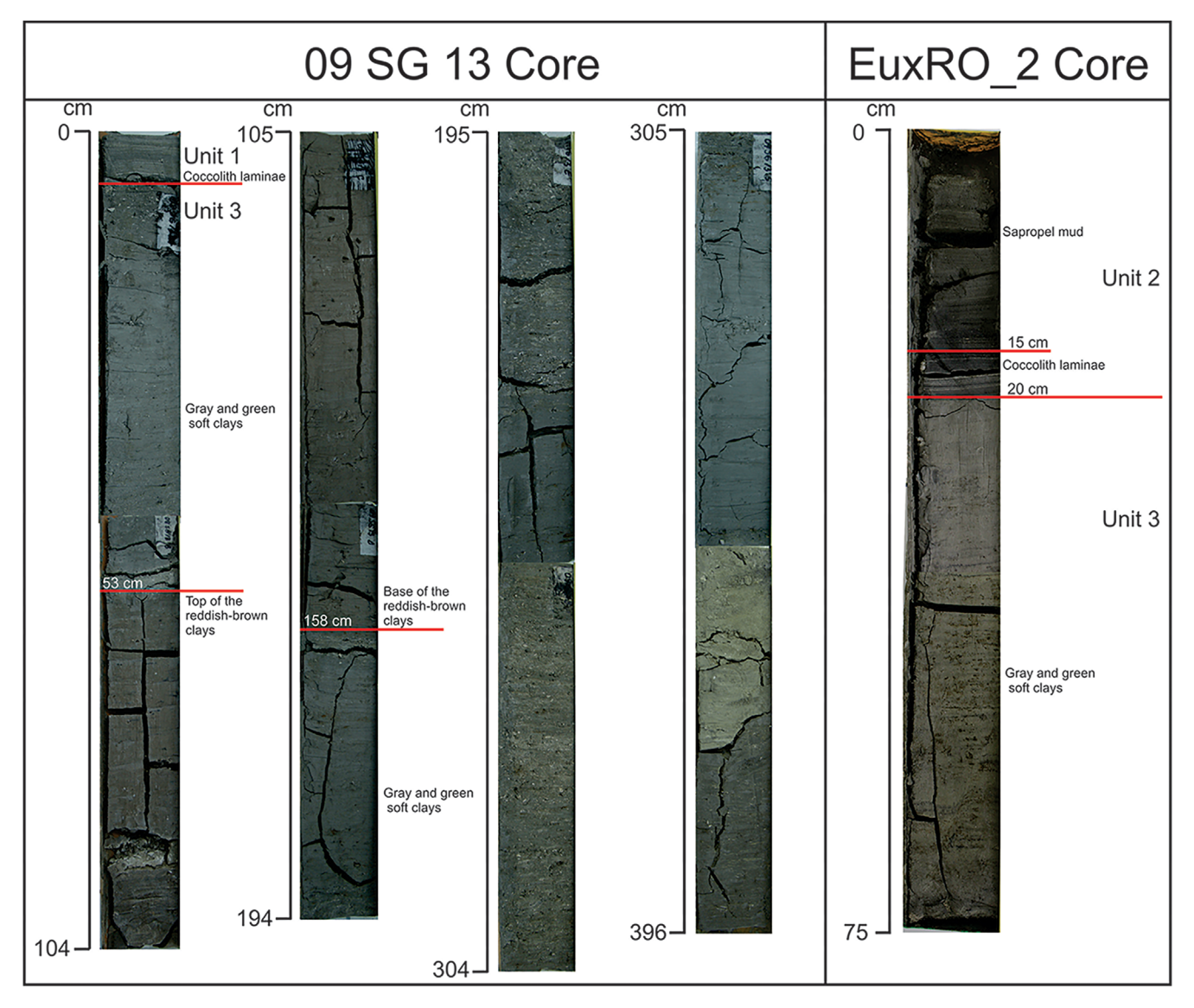


Figure 2. Photographs of the studied cores (09 SG 13 and EuxRO\_2) illustrating the main lithological units and the distribution of the reddish-brown clay interval.

Reference materials used for identification follow Schornikov (1964, 2011), Olteanu (1978), Stancheva (1989), Boomer et al. (2003, 2010), Ivanova et al. (2007), Opreanu (2008) and Zenina et al. (2017).

### Chronology

<sup>14</sup>C age determinations were undertaken on four samples from core 09 SG 13 at the NOSAMS Facility at Woods Hole Oceanographic Institution, on juvenile valves of the mollusk *Dreissena rostriformis*. <sup>14</sup>C dates were measured at 13, 59, 159 and 389 cm below the sea floor (bsf). Some of these depths correspond to lithological boundaries in the core: (i) 389-159 cm bsf refers to gray clay, (ii) 159-59 cm bsf refers to red clay, (iii) 59-13 cm bsf refers to light gray clay, and (iv) the top 13 cm bsf refers to white clay. The  $^{14}\text{C}$  ages at these boundaries are 24 500  $\pm$  280, 15  $000 \pm 50$ , 13  $800 \pm 45$  and 11  $100 \pm 40^{-14}$ C a BP, respectively. The ages between these 14C-dated intervals are linearly interpolated. The <sup>14</sup>C reservoir ages applied are taken by tuning the  $\delta^{18}O$  and  $\delta^{13}C$  composition of the Black Sea mollusk record to the U/Th-dated  $\delta^{18}$ O and  $\delta^{13}$ C composition of Sofular Cave (Fleitmann et al., 2009; Badertscher et al., 2011) for the deglacial period with the applied calibration of Reimer et al. (2013) to calculate the <sup>14</sup>C reservoir ages (Reimer et al., 2013; Yanchilina et al., 2017, 2018). The calibration was done directly between calendar ages and Northern Hemisphere 14C atmospheric ages as a linear regression between points where the Northern Hemisphere 14C atmospheric age isobserved to vary linearly as a function of calendar age. Yanchilina et al. (2018) document the specific steps of the calibration and <sup>14</sup>C reservoir calculation. Sofular Cave is located in northern Turkey, close to the Black Sea coast, and tracks the isotopic signature of Black Sea surface water, allowing a reconstruction of the precise timing of hydrological shifts of the basin (Badertscher et al., 2011). The corresponding calendar ages are 28 500-24 500, 16 350-15 000, 15 150-13 800 and 12 850-11 100 a (Table 1; Fig. 3). To allow correlation with previously published data grom several authors (Boomer et al., 2010; Lericolais et al., 2010; Ivanova et al., 2012), the uncalibrated radiocarbon dates are used in this paper, with corresponding calendar age for each date (Table 1).

### Stable isotopes

Stable isotope measurements were undertaken at Rutgers University (Department of Earth and Planetary Sciences) by gas-sourced mass spectrometry on 51 samples from core 09 SG 13. Approximately 700–1200  $\mu g$  per sample of shell material (ostracod valves and carapaces) was used. The errors are 0.06% for  $\delta^{18}$ O. Here we use the  $\delta^{18}$ O isotope curve published by Briceag *et al.* (2016). The  $\delta^{18}$ O isotopes were measured on juvenile *D. rostriformis* shells for a surface water proxy signal and on Candonidae ostracod valves for the deeper water signal.

### Inorganic CaCO<sub>3</sub> and organic matter

To determine the total carbonate content and organic matter, loss on ignition was determined every 10 cm for core 09 SG 13 and every 5 cm for EuxRO\_2, by using a furnace Snol 8.2/1100. In total, 41 samples were used for core 09 SG 13 and 15 for EuxRO\_02. Studies were performed in the National Institute for Marine Geology and Geo-ecology, Bucharest.

### **Results**

### Chronostratigraphy

The age model of core 09 SG 13 is based on <sup>14</sup>C ages of juvenile *D. rostriformis*. The lithological unit between 24 500 and 15 000 <sup>14</sup>C a BP is placed in the latter part of Marine Isotope Stage 2 (MIS 2). The lithological unit between 15 000 and 13 800 <sup>14</sup>C a BP reflects the meltwater event occurring concurrent with the Heinrich Event 1 (Bahr *et al.*, 2005; Major *et al.*, 2006; Soulet *et al.*, 2011a,b).

To supplement the <sup>14</sup>C dating of the core, the CaCO<sub>3</sub> content of the sediments of both cores was used to identify the time periods represented by the lithological units. The changes in CaCO<sub>3</sub> in the Black Sea sediments are thoroughly dated and provide a clear age control (Ryan *et al.*, 2003; Bahr *et al.*, 2005, 2006, 2008; Major *et al.*, 2006; Ryan, 2007). The high carbonate content in copre 09 SG 13 between 13 800 and 11 100 <sup>14</sup>C a bp represents the Bølling–Allerød warming. The high carbonate content in the top 13 cm of core 09 SG 13 is assumed to represent the warm and stable Upper Holocene.

The sediment accumulation rate (SAR, cm ka $^{-1}$ ) was calculated in core 09 SG 13 for the last 24 000  $^{14}$ C a BP. Values range from 17 to 83.3 cm ka $^{-1}$ . For the oldest part of the core (360–160 cm bsf, from 24 000 to 15 000  $^{14}$ C a BP) the SAR values are relatively low, 24.2 cm ka $^{-1}$ . Above this interval (160–60 cm bsf, between 15 000 and 13 800  $^{14}$ C a BP), during the period of reddish-brown clay deposition, the SAR values show an almost four-fold increase, to 83.3 cm ka $^{-1}$ . Between 60 and 14 cm bsf (from 13 800 to 11 000  $^{14}$ C a BP), an extremely low SAR is observed, *i.e.* 17.0 cm ka $^{-1}$ .

### Lithology and macrofauna of core 09 SG 13

In core 09 SG 13, two lithological units, as identified by Ross and Degens (1974) for the deep parts of the Black Sea, have been recognized: Unit 3 (the oldest) and Unit 1 (the youngest). As Unit 2, the Sapropel Mud was not identified in this core, and Unit 1 overlies Unit 3, a hiatus could be assumed between Units 1 and 3.

From the base of the core, *i.e.* 396 cm bsf, up to 158 cm bsf, the lithology consists of gray and green soft clays with specks of iron sulfide (FeS), fine silicic laminae and fine sand intercalations, millimeters up to centimeters thick (Briceag *et al.*, 2016). Above this, between 158 and 53 cm bsf, are reddish-brown clays with centimeters-thick sands (Figs 2 and 3). Between 145 and 130 cm bsf, a gray mud intercalation was observed in the reddish-brown clays. The

Table 1. Radiocarbon data and calendar ages of core 09 SG 13. For the calibration, the IntCal09 calibration curve was used.

Sample depth (cm)	Material	<sup>14</sup> C age (a BP)	Laboratory number	Corresponding calendar age (a BP)	<sup>14</sup> C age error (a BP)
13	Dreissena rostriformis	11 100	OS-106842	12 850	40
59	Dreissena rostriformis	1380	OS-106843	15 150	45
159	Dreissena rostriformis	15 000	OS-106888	16 350	50
389	Dreissena rostriformis	24 500	OS-106887	28 500	280

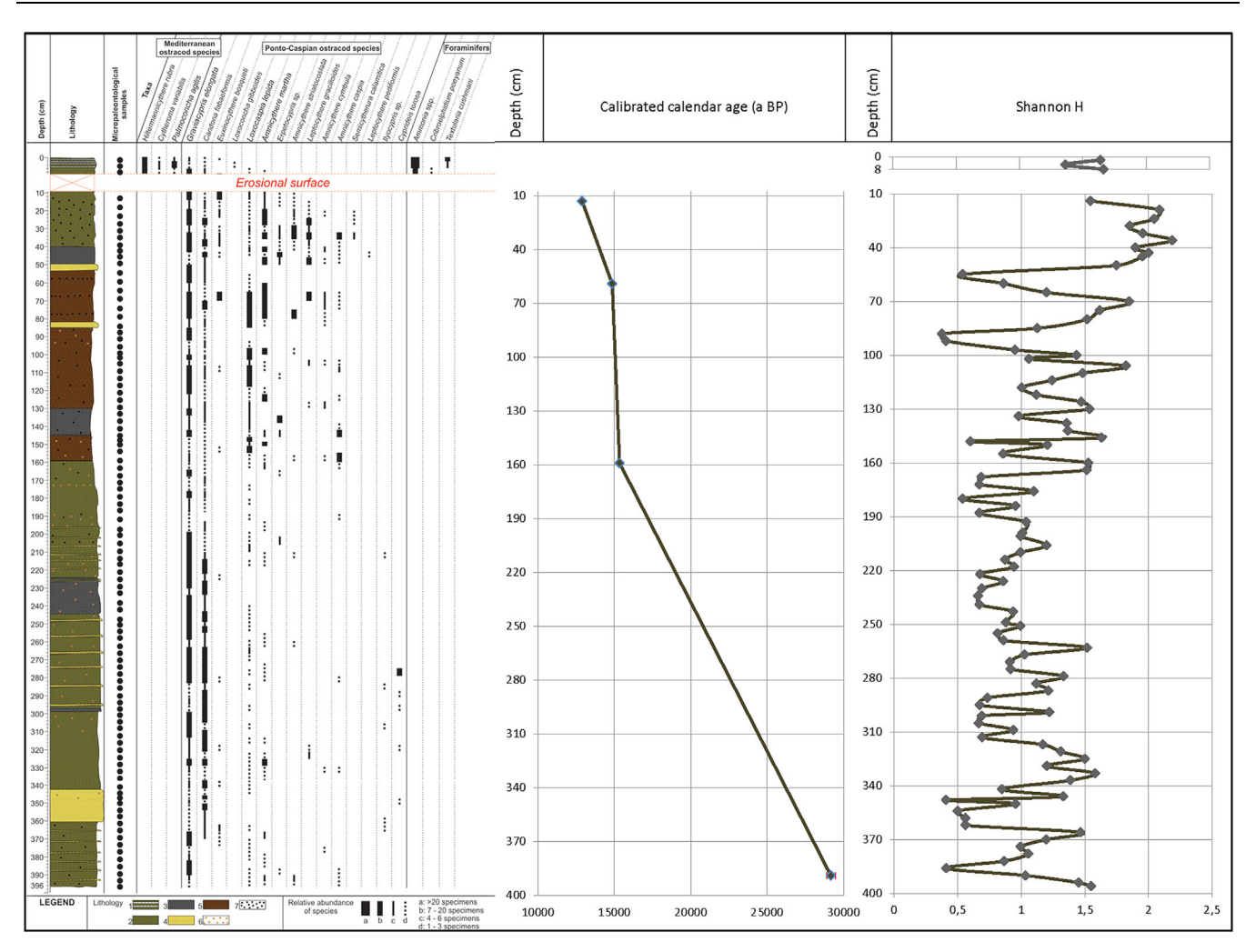


**Figure 3.** Lithology and microfaunal (ostracods and foraminifers) distribution and abundance in core 09 SG 13 (left side). Lithology: 1 – greenish gray silty clays with fine coccolith laminae intercalations; 2 – greenish gray silty clays; 3 – gray silty clays; 4 – fine silty sands; 5 – reddish-brown clay; 6 – FeS and iron oxides; 7 – organic matter. Relative abundance of species: a – abundant; b – frequent; c – moderate; d – rare. Age–depth plot and diagram show Shannon H ostracod diversity indices for core 09 SG 13.

youngest deposits of Unit 3, between 53 and 8 cm bsf, are composed of gray and green soft clays with black specks of organic matter (Briceag *et al.*, 2016). Many layers of Unit 3 contain bivalves, mostly *D. rostriformis*, and gastropod shells.

The youngest 7 cm bsf of the core is composed of gray and green silty clays, interbedded with millimeter-scale coccolith laminae (Figs 2 and 3) (Briceag *et al.*, 2016). Towards the base of Unit 1, in the interval 5–6 cm bsf, a coquina layer, containing *Modiolus phaseolinus* and *Mytilus galloprovincialis*, has been identified.

### Lithology and macrofauna of core EuxRO 2

In core EuxRO\_2, two lithological units have been recognized: Unit 3 and Unit 2. The absence of Unit 1 is due to either downslope gravitational sliding or non-deposition.

From 70 to 20 cm bsf, the lithology consists of homogenous gray and green clays with black specks of organic matter and high content of fine pyrite particles. From 70 to 42 cm bsf, gypsum crystals are present. The uppermost 20 cm contains dark, fine-grained sediments with high organic content, *i.e.* the sapropel mud of Unit 2 (Figs 2 and 4). Between 20 and 15 cm bsf millimeter-scale coccolith laminae are present in Unit 2 (Figs 2 and 4).

With regard to the macrofauna, shell fragments of *D. rostriformis* bivalves and microgastropods were identified,

between 70 and 20 cm bsf. The uppermost 20 cm bsf contains only a few larval stages of bivalves and microgastropods, along with fish bones and otoliths.

### Inorganic CaCO<sub>3</sub> and organic matter content of core 09 SG 13

Inorganic CaCO<sub>3</sub> values are between 2.1 and 15.2%. Based on its fluctuation, three intervals can be separated in core 09 SG 13, as follows (oldest first): (i) from the base of the core, between 396 cm bsf and up to 200 cm bsf, inorganic CaCO<sub>3</sub> values are between 5.0 and 7.3%; (ii) from 200 cm bsf up to the top of the reddish-brown clays (i.e. 53 cm bsf), values decrease to between 2.1 and 3.5%; and (iii) from the top of the reddish-brown clays to the top core, CaCO<sub>3</sub> values increase to 14.0% (at 32 cm bsf), and to a maximum of 15.2% (at 7 cm bsf) in the lowermost part of Unit 1.

Organic matter (OM) values are between 2.4 and 9.3%. From 381 cm bsf up within the core, OM values decrease from 7.5 to 2.7% (at 354 cm bsf). Above this, OM values shift to 8.2%, with values over 6% up to 312 cm bsf; upwards, OM values are again are lower, i.e., 2.4% at 262 cm bsf. Another increase in OM is recorded at 242 cm bsf, to 6.3%. Between 222 and 204 cm bsf, the OM values are low, 3–4%. In interval 192–102 cm bsf, OM values are high, between 5.5 and 7%. From 92 to 7 cm bsf, OM values oscillate between 4.2% (at 92 cm bsf) and 7.7% (at

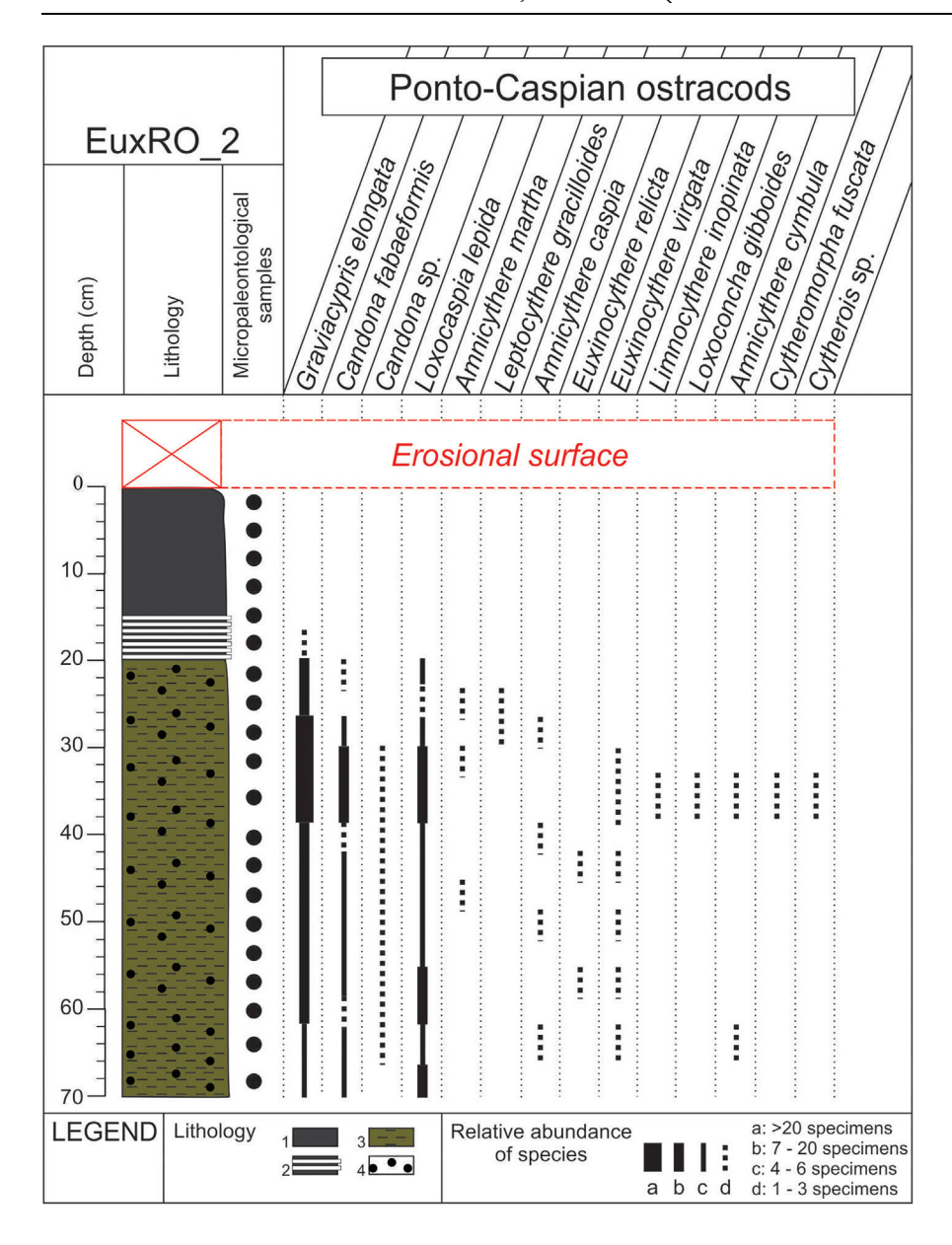


**Figure 4.** Lithology and microfaunal (ostracods) distribution and abundance in core EuxRO\_2 core. Lithology: 1 – sapropel; 2 – sapropel with fine coccolith laminae intercalations; 3 – greenish gray silty clays; 4 – organic matter. Relative abundance of species: a – abundant; b – frequent; c – moderate; d – rare.

42 cm bsf). The peak OM value is 9.3%, recorded in the youngest Unit 1, at 3 cm bsf.

### Inorganic CaCO<sub>3</sub> and organic matter content of core EuxRO 2

Inorganic CaCO<sub>3</sub> values for core EuxRO\_2 are between 2.74 and 18.65%. From 70 to 55 cm bsf, values are between 2.74 and 3.42%. From 50 to 20 cm bsf, CaCO<sub>3</sub> increases, to between 8.37 and 18.65%. From this interval to the uppermost part of the core, in the sapropel, the CaCO<sub>3</sub> content progressively decreases, down to 3.55%.

OM values are between 6.37 and 35.04%. From 70 to 20 cm bsf, OM values oscillate between 6.37 and 12.18%. From 20 cm bsf to the uppermost part of the core, in the sapropel, the OM values are very high, reaching a maximum of 35.04% at 15 cm bsf.

### Ostracod assemblages

Quantitative and qualitative studies have been made for both cores, 09 SG 13 and EuxRO\_2 (Fig. 5). For core 09 SG 13, values of the Shannon H index have been plotted against core depth to reveal variations in ostracod diversity (Fig. 3).

The Shannon H index varies from 0.38 (88 cm bsf) to 2.18 (36 cm bsf). Six ostracod assemblages were distinguished in cores 09 SG 13 and EuxRO\_2 based on the changes in microfossil taxa, and these are stratigraphically important. These are as follows (oldest first):

Assemblage 6 (396-160 cm bsf; 09 SG 13) is represented by high abundance of Candonidae species (up to 20 specimens/ sample), Graviacypris elongata and Candona fabaeformis. Other species present in this interval, at lower abundances, are Euxinocythere bosqueti, Loxocaspia lepida, Amnicythere martha, A. striatocostata, A. cymbula, A. caspia, Erpetocypris sp., Leptocythere gracilloides, Ilyocypris gibba and Cyprideis torosa (up to eight specimens/sample; Briceag et al., 2016). Between 396 and 390 cm bsf, Leptocytheridae are dominant, i.e. 60% of the total assemblage (Figs 3 and 5). The Shannon H diversity index displays a sharp decrease (Fig. 3) from 1.55 (396 cm bsf) to 1.03 (390 cm bsf). Above this, between 390 and 160 cm bsf, the abundance of Candonidae increases, Leptocytheridae decreases, while Loxoconchidae show similar values. In this interval, the Shannon H diversity index shows very strong variation (Fig. 3), from 0.41 (348 cm bsf) to 1.58 (333 cm bsf). The 370 cm bsf core interval is characterized by the appearance of *C. fabaeformis* (Fig. 3).

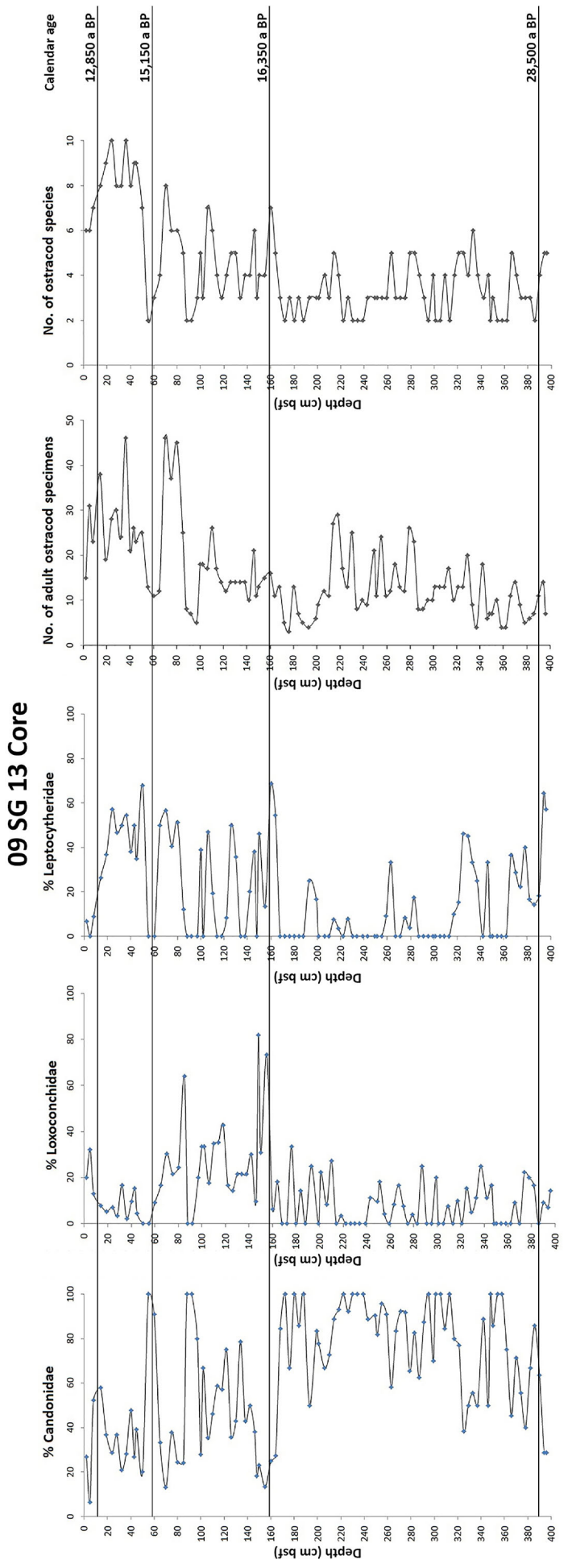
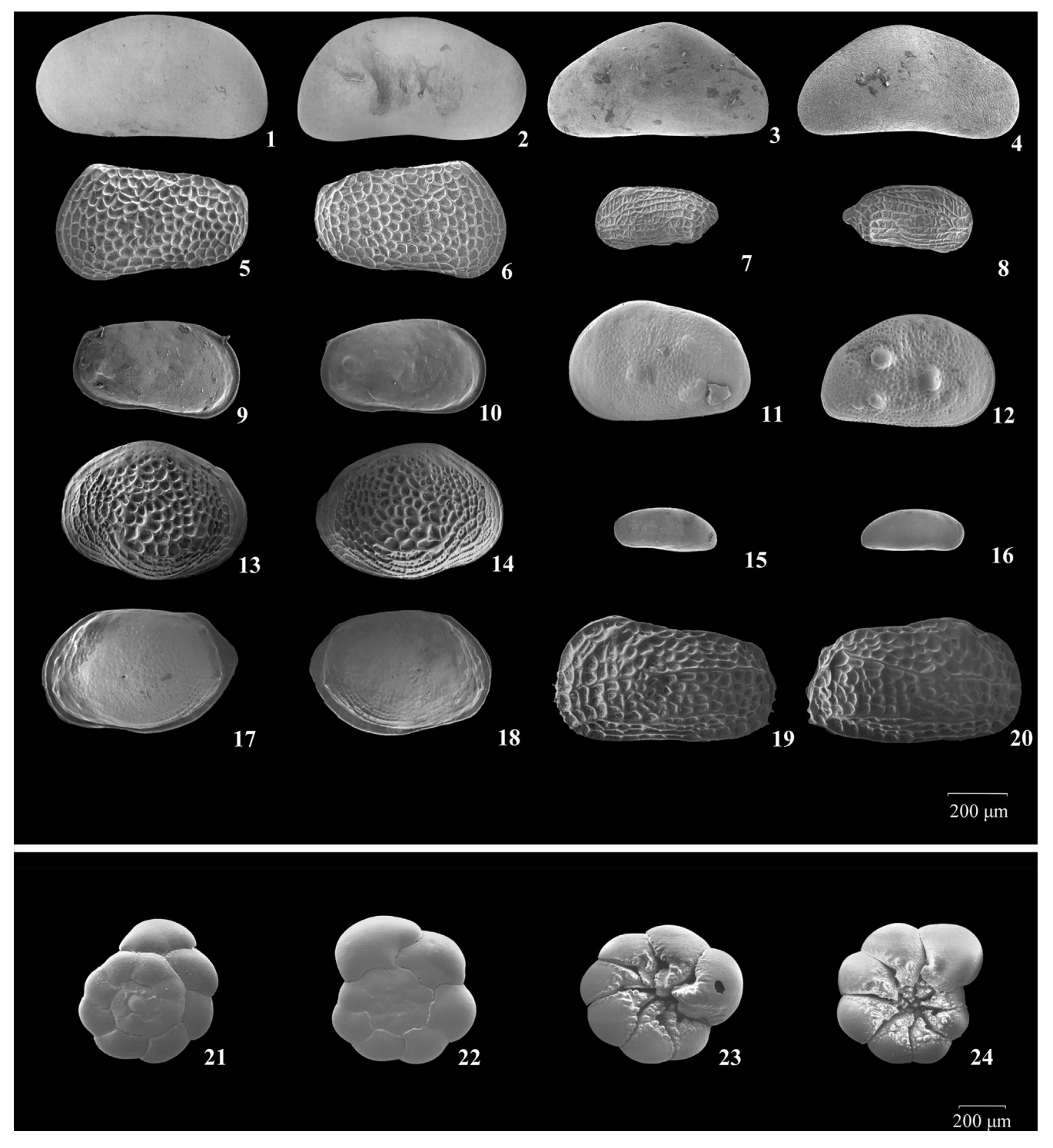


Figure 5. Fluctuation in ostracod abundance (% of the main ostracod groups and of all adult specimens), diversity (number of species/sample) and calibrated calendar age.



**Figure 6.** Scanning electron micrographs of ostracods and foraminifers identified in core 09 SG 13. All ostracod valves belong to adult individuals, except 11 and 12 (juvenile individuals), external lateral views; LV=left valve, RV=right valve. 1, 2: *Graviacypris elongata* (Schweyer): 1 – LV; 2 – RV; 3, 4: *Candona fabaeformis* (Fischer): 3 – LV; 4 – RV; 5, 6: *Amnicythere martha* (Livental): 5 – LV; 6 – RV; 7, 8: *Semicytherura calamitica* Schornikov: 7 – LV; 8 – RV; 9, 10: *Amnicythere cymbula* (Livental): 9, 10 – RV; 11, 12: *Cyprideis torosa* (Jones): 11 – LV; 12 – RV; 13, 14: *Loxoconcha gibboides* Livental: 13 – LV; 14 – RV; 15, 16: *Cytheroma variabilis* Müller: 15 – LV; 16 – RV; 17, 18: *Palmoconcha agilis* (Ruggieri): 17 – LV; 18 – RV; 19, 20: *Hiltermannicythere rubra* (Müller): 19 – LV; 20 – RV; 21–24: *Ammonia tepida* (Cushman): 21, 22 – spiral view; 23, 24 – umbilical view.

Assemblage 5 (160–55 cm bsf; 09 SG 13) is defined by high abundances of *L. lepida*, *A. martha* and *A. caspia* species (up to 16 specimens/sample). Diversity increases along with the abundance of Loxoconchidae and Leptocytheridae, overlapping the Candonidae. The Shannon H diversity index displays strong variation (Fig. 3), with the highest value of 1.84 (70 cm bsf). The lowest value of diversity is recorded (0.38 at 88 cm bsf) in this assemblage. The abundance peak in the Loxoconchidae and

Leptocytheridae, each at around 70% of the total assemblage, is found at the base of the reddish-brown clays (between 160 and 140 cm bsf). In this depositional interval, the Candonidae show a sharp drop, below 20% (Fig. 5). Above this, their abundance increases, reaching a peak of 100% at 55 cm bsf (the top of the reddish-brown clays).

Assemblage 4 (55–7 cm bsf; 09 SG 13) is characterized by high diversity and abundance, up to 20 specimens/sample. It contains commonly *G. elongata, C. fabaeformis, A. martha,* 

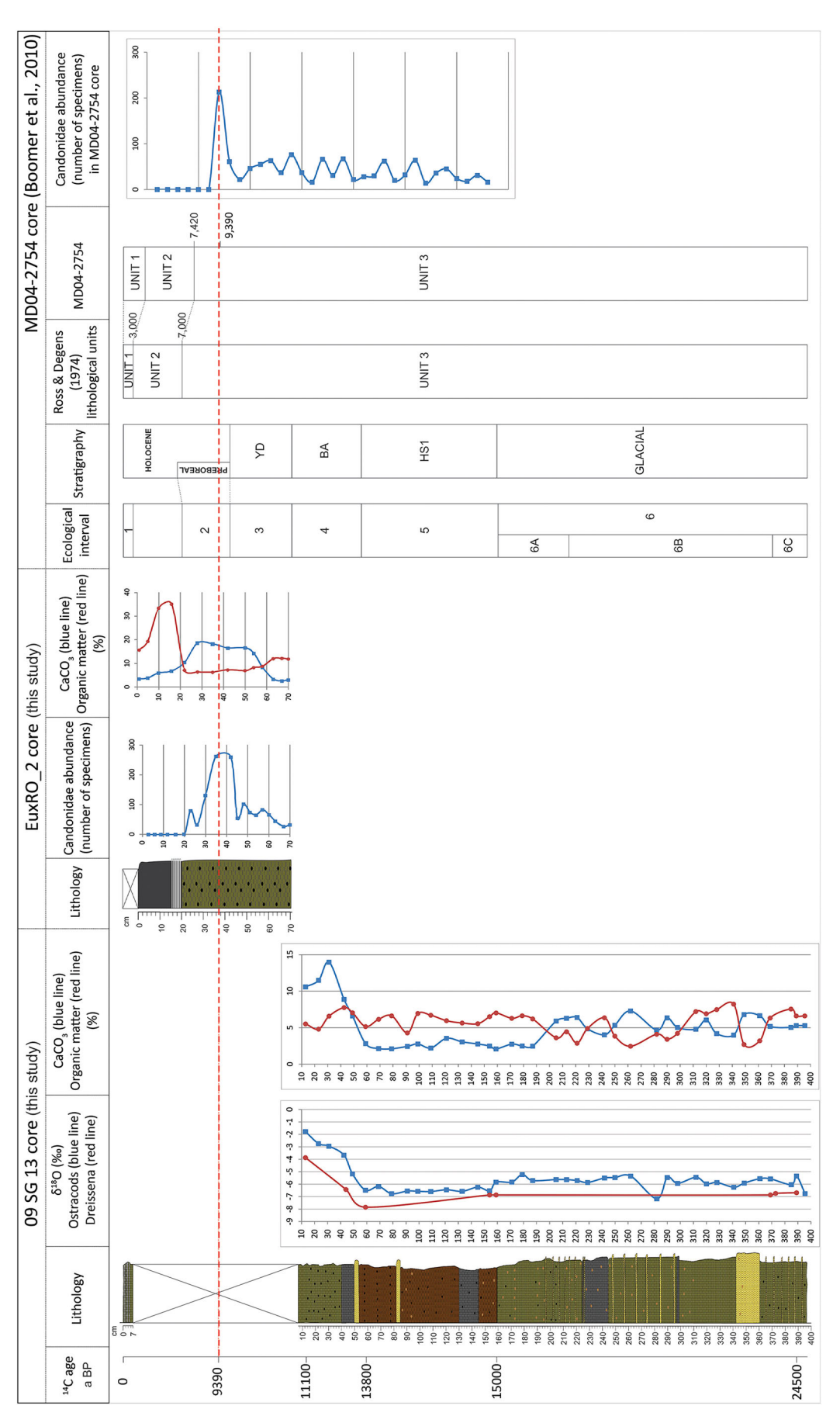


Figure 7. Correlation between the obtained data (from cores 09 SG 13 and EuxRO\_2) and the classical units of Ross and Degens (1974), as well as core MD04-2754 of Boomer et al. (2010) along with 8\displays Solope, organic matter and CaCO<sub>3</sub> fluctuations during the last 25 000 a bp. HS1: Heinrich Stadial 1; BA: Böllling–Alleröd; YD: Younger Dryas.

A. striatocostata and L. gracilloides (Fig. 3). The Shannon H diversity index shows a strong increase (Fig. 3), recording the highest value of diversity (2.18 at 36 cm bsf).

Assemblage 3 (70–42 cm bsf; EuxRO\_2) is characterized by low diversity and abundance (Figs 5 and 6). The most abundant ostracods are *L. lepida* and *G. elongata. L. lepida* dominates the lower part of this interval (up to 40 specimens/sample), between 70 and 57 cm bsf, while *G. elongata* dominates the upper part (up to 70 specimens/sample).

Assemblage 2 (42–20 cm bsf; EuxRO\_2) shows a four-fold increase in Candonidae and Loxoconchidae abundance, up to 200 specimens/sample. In this interval, maximum diversity (10 species) in the core (the uppermost 70 cm) was observed (Figs 5 and 6).

Assemblage 1 (from 7 cm bsf to the top; 09 SG 13) is represented by high abundances of the marine taxa *Hilter-mannicythere rubra, Cytheroma variabilis* and *Palmoconcha agilis* (Figs 3 and 6). The highest abundance is recorded by *Hiltermannicythere rubra,* 15 specimens/sample. Other ostracods in this interval that are present at low abundance, are *G. elongata, E. bosqueti, Loxoconcha gibboides, L. lepida* and *A. martha.* The Shannon H diversity index displays stable values (Fig. 3), between 1.36 (5 cm bsf) and 1.64 (2 cm bsf).

### Foraminiferal assemblages

The foraminiferal assemblages of the top 7 cm of core 09 SG 13 contain well-preserved benthic foraminifers, such as *Ammonia* spp., *Cribroelphidium poeyanum* and *Textularia cushmani* (Figs 3 and 6). In Unit 3, *i.e.* from 396 to 7 cm bsf, no *in situ* foraminiferal taxa were identified. *Ammonia* spp. in Unit 1 dominates the assemblage, showing high abundances, up to 380 specimens/sample (Fig. 6). The abundance of *T. cushmani* is high in the uppermost part of Unit 1, *i.e.* up to 14 specimens/sample, but decreases towards the base of this unit to three specimens/sample. The abundance of *C. poeyanum* is very low everywhere. In EuxRO\_2, only few

reworked *Ammonia* spp. juvenile specimens were encountered in Unit 2. The presence of a scarce assemblage is probably linked to the anoxic environment of Unit 2, the sapropelic mud. The assumption that they are reworked is based on the poor state of preservation and the low number of specimens.

### Discussion

Benthic ostracods are highly sensitive to salinity and temperature changes, therefore indicating (paleo)environmental fluctuations. Numerous studies have used ostracods as proxies to reconstruct paleoenvironments of the Holocene from the Black Sea, also focusing on the taxonomy of this group of organisms. For instance, Boomer *et al.* (2010) published a taxonomic summary of the most abundant Black Sea ostracods occurring within the Lateglacial to Early Holocene interval. The authors highlighted issues regarding the taxonomy of the ostracods from the Ponto-Caspian region. Zenina *et al.* (2017) made a revision to the ostracod taxonomy published by Ivanova *et al.* (2007) from core Ak-521 (NE Black Sea; Fig. 1), by Ivanova *et al.* (2015) from core Ak-2575 (NE Black Sea; Fig. 1) and recent fauna of Caspian type found by Opreanu (2008) in the Romanian shelf.

In both cores EuxRO\_2 (NW Black Sea shelf, 500 m water depth) presented herein and core MD04-2754 studied by Boomer *et al.* (2010) (SW Black Sea shelf, 453 m water depth; Fig. 1) the presence of Ponto-Caspian ostracod assemblages dominated by *Graviacypris elongata* just below the Sapropel Mud is reported (Fig. 7). The absence in both cores of Mediterranean taxa below the Sapropel Mud may be related to the low paleosalinity of this area. Concerning other microfaunal groups of organisms, Yanko-Hombach *et al.* (2017) presented a chart showing that benthic foraminiferal diversity diminished with decreasing salinity in various areas of the Black Sea, from the Bosphorus (in the south) towards the Danube Delta mouth (in the north).

**Table 2.** Faunal type (M, species of Mediterranean type; C, species of Caspian type), along with ecological affinities of the identified ostracod species based on literature data, and ecological interval classification.

Name of species	Faunal type	Ecological affinity	Ecological interval
Palmoconcha agilis	М	Polyhaline	1
Cytheroma variabilis	M	Polyhaline	1
Hiltermannicythere rubra	M	Mesohaline	1
Graviacypris elongata	C	Oligohaline	6, 5, 4, 3, 2, 1
Candona fabaeformis	С	Oligohaline	6, 5, 4, 3, 2, 1
Candona sp. 3 sensu Boomer et al. (2010)	С	Oligohaline	3, 2
Euxinocythere bosqueti	С	Mesohaline	6, 5, 4, 1
Euxinocythere relicta	С	Oligohaline to mesohaline	3
Euxinocythere virgata	С	Mesohaline	3, 2
Loxoconcha gibboides	С	Oligohaline	2, 1
Loxocaspia lepida	С	Oligohaline	6, 5, 4, 3, 2, 1
Amnicythere martha	С	Mesohaline	6, 5, 4, 3, 2, 1
Erpetocypris sp.	С	Oligohaline to mesohaline	6, 5, 4
Amnicythere striatocostata	С	Oligohaline to mesohaline	6, 5, 4
Leptocythere gracilloides	С	Oligohaline	6, 5, 4, 2
Amnicythere cymbula	С	Oligohaline	6, 5, 4, 3, 2
Amnicythere caspia	С	Oligohaline	6, 5, 4, 3, 2
Leptocythere pediformis	С	Oligohaline to mesohaline	4
Cytheromorpha fuscata	С	Oligohaline to mesohaline	2
Cytherois sp.	С	Mesohaline	2
Limoncythere inopinata	C	Freshwater to mesohaline	2
Ilyocypris sp.	C	Freshwater to oligohaline	6
Cyprideis torosa	Č	Holeuryhaline	6
Semicytherura calamitica	Č	Mesohaline	4

Ecological affinity after Opreanu (2006), Boomer et al. (2010), Ivanova et al. (2012) and Bony et al. (2015).

Studies based on dinocysts (Mudie et al., 2007; Marret et al., 2009) concluded that before the connection with the Mediterranean, salinity in the Black Sea fluctuated between 5 and 12‰. Mertens et al. (2012) agree with this assumption and suggest that, after reconnection, salinity was also low, i.e. between 13 and 15%. Williams et al. (2018) document the replacement of Ponto-Caspian ostracod assemblages by Mediterranean species from two cores acquired from the SW Black Sea shelf. The authors estimate a salinity of  $\sim$ 5-10% between 11 910 and 7425 a BP, followed by an increase in salinity to  $\sim 13-15\%$  from  $\sim$ 7425 to 6310 a BP, when they recorded the first Mediterranean ostracod species. Zenina et al. (2017) identify on the NE Black Sea shelf (~100 m water depth), on the Caucasian outer shelf, the first appearance of Mediterranean ostracod species at ~9600 cal a BP. Ostracod assemblages comprising only Mediterranean species were found in the NE Black Sea in a deposition interval younger than 6800 a BP (Zenina et al., 2017). In summary, the above studies indicate that before the Black Sea - Mediterranean connection, salinity was between 5 and 12% and after reconnection was higher, i.e., 13-15%.

Similar results are shown by our investigation. Hence, in the youngest sediments of core 09 SG 13, *i.e.* Unit 1 (Coccolith Mud), both Mediterranean and Ponto-Caspian ostracod species occur. The percentage of Mediterranean taxa is higher, 65%. We assume that salinity increased during the latest Holocene, but was still low, probably up to 15‰, supporting the survival of Ponto-Caspian taxa.

The sampled interval from core EuxRO\_2 covers the latter part of the Younger Dryas, the whole Preboreal warming period and the Lower Holocene interval (Fig. 7). We assume that the absence of Unit 2 from core 09 SG 13 is related to the existence of a sharp density contrast between the fresh water and the underlying saltier water (Ryan, 2007). Hence, a significant density change would allow internal waves to migrate across the interface. These waves braked against the seabed around the entire basin margin, including the upper slope - outer shelf areas (Ryan, 2007). Such waves triggered or amplified by large storms and/or earthquakes would wash the seabed and remove the superficial sediments, including the sapropel of Unit 2 and the clays of the upper part of Unit 3. The washout at the Unit 3 – Unit 2 boundary is observed in many Black Sea cores (Khrischev and Georgiev, 1991), probably related to the aforementioned phenomenon.

Paleoclimatic changes during these periods are reflected not only in the sedimentary record, but also in the microfauna. Hence, based on abundance and diversity of the ostracod assemblages, six ecological intervals are described from the core 09 SG 13 and uppermost 70 cm of core EuxRO\_2, corresponding to shifts in climate and salinity (Fig. 7).

### Ecological interval 6

This was observed in Unit 3 and it is represented by ostracod assemblages showing relatively low abundance and diversity (Figs 5 and 6). The ostracods are fresh to brackish taxa that prefer salinities between 5 and 8‰, considering the maximum values of salinity allowing survival of *G. elongata* and *C. fabaeformis* (Schornikov, 1964; Ivanova *et al.*, 2007), the most abundant species found within this interval. These ostracods inhabit the present-day Caspian Sea basin, where salinity is not higher than 14‰ (Stancheva, 1989; Schornikov, 2011). Based on the ostracod assemblages, Ecological interval 6 may be divided in three sub-intervals (Fig. 7; Table 2):

- i. Subinterval 6C covers the base of the core, e. 396–370 cm bsf. It contains high ostracod diversity, arguing for abundant nutrient supply. The presence of the warm water species *Erpetocypris* sp., at very low abundances (i.e., one specimen), suggests uniform temperatures, above freezing.
- ii. Subinterval 6B, between 370 and 214 cm bsf, is marked by the occurrence of cold water species. The high abundance and continuous presence of C. fabaeformis implies a decrease in bottom water temperature. C. fabaeformis is known today to inhabit low-temperature waters of the Siberian lakes (Konovalova, 2016). Another cold water taxon of this subinterval, I. gibba, is encountered in western Siberia Pleistocene deposits (Konovalova, 2015). This is in accordance with the  $\delta^{18}$ O record, corresponding to MIS-2, and CaCO3 values that are homogenous and relatively low (Fig. 7). Between 350 and 277 cm bsf the Caspian ostracod C. torosa (Schornikov, 2011; Briceag et al., 2012) is found. This may be related to a temporal overflow of Caspian water into the Black Sea. This agrees with Qin and Yu (1998), who reported that around 18 000 a BP the Caspian Sea surface expanded. Chepalyga (2007) dates the Khvalynian transgression of the Caspian Sea to between 17 000 and 14 000 a BP. The other ostracod species present in this subinterval have relatively low abundance; many of these taxa inhabit the present-day Danube Delta lakes, where temperatures decrease significantly in winter; these species tolerate low temperatures (including in frozen lakes).

Possibly, the Black Sea surface was partially covered by ice in this subinterval, at least on its shelf. A frozen lake hypothesis explains the occurrence of sand intercalations without mud, probably related to glacier type transportation, allowing transport of sand from the beach to the far offshore in ice (i.e. ice-rafted debris). Additionally, an eventually cold interval is supported by the occurrence of C. torosa, an ostracod that tolerates temporary freezing (Meisch, 2000). Concomitantly,  $\delta^{18}O$  values drop significantly (Fig. 7). Additionally, the relatively low sedimentation rate is possibly linked to low sediment influx in this area and frozen rivers. This subinterval corresponds to HS-2, a period with colder and drier conditions coupled with low continental hydrological input (Soulet et al., 2011a). Moreover, the  $\delta^{18}O$  record of Sufular Cave (northern Turkey) tracks the isotopic signature of Black Sea surface water, and allows a reconstruction of the precise timing of hydrological shifts of the Black Sea (Badertscher et al., 2011). U/Th-dated stalagmites (Fleitmann et al., 2009; Badertscher et al., 2011) reveal an interval of non-precipitation in the stalagmite columns during HS-2. Non-precipitation caused by the presence of overlying permafrost is compatible with a Black Sea partially covered by ice.

iii. Subinterval 6A from 214 to 158 cm bsf is marked by the disappearance of the cold water taxon *I. gibba* and decreased abundance of *C. fabaeformis*. These bioevents probably imply a slight increase in bottom water temperature, supported by the reappearance of the warm water ostracod *Erpetocypris* sp.

### Ecological interval 5

This interval encompasses the time-span of deposition of the reddish-brown clay, corresponding to the Fennoscandian Ice Sheet meltwater pulse (i.e. beginning 15 000–13 800 <sup>14</sup>C a BP) (Briceag *et al.*, 2016). The increases in ostracod diversity

and abundance, compared with the LGM interval, suggest higher nutrient delivery to the basin (Briceag et al., 2016). The occurrence at high abundance of oligonaline ostracods L. lepida and A. cymbula (Table 2) throughout this interval suggests a shift in salinity from 5-8% to 0.5-5% (Ivanova et al., 2007). L. lepida today inhabits shallow deltas, lagoons and estuaries with very low salinity (Opreanu, 2008).  $\delta^{18}$ O isotope and CaCO<sub>3</sub> values show decreases (Fig. 7), possibly due to the seasonal northern high influx of fresh water into the basin (Major et al., 2006; Soulet et al., 2011a). The fresh water influx is reflected in the four-fold sedimentation rate increase compared with the LGM and the occurrence of exclusively freshwater ostracod fauna along with L. lepida and A. cymbula development. Based on pollen data, Shumilovskikh et al. (2012) show that warming and humidity increase during melt-water pulses in the Black Sea.

### Ecological interval 4

This interval is marked by very high abundance and diversity of the ostracod assemblages along with the re-occurrence of the warm water taxon Erpetocypris sp. (Fig. 3). This interval corresponds to the Bølling-Allerød warm period. Boomer et al. (2010) document ostracod abundance and diversity from core MD04-2754 (NW Black Sea shelf, 453 m water depth; Fig. 1), which show similarities with our data from core 09 SG 13. The high δ<sup>18</sup>O isotope and CaCO<sub>3</sub> values, increasing significantly together with high ostracod abundance and diversity, indicate enhanced primary productivity at the onset of the Bølling-Allerød warm period (Bahr et al., 2008; Figs 5 and 7). After this warm period, a cold and dry climate prevailed during the Younger Dryas stade (Lericolais et al., 2009), which led to the decrease in ostracod abundance and diversity, along with the disappearance of the warm water taxon Erpetocypris sp.  $\delta^{18}$ O isotope values increased slightly during the Younger Dryas cold interval. The sedimentation rate is extremely low, due to soil development and increased vegetation cover in the catchment area of the Black Sea, an event that began in the Bølling-Allerød warm interval (Kwiecien et al., 2008).

### Ecological interval 3

This interval corresponds to the end of the Younger Dryas cold period, being characterized by the transition from ostracod assemblages dominated by the oligohaline species *L. lepida* to assemblages dominated by *G. elongata* (Table 2). This change indicates a slight increase in salinity at the end of the Younger Dryas.

### Ecological interval 2

Candonidae and Loxoconchidae taxa increase four-fold in abundance. During this interval, the highest ostracod diversity in the studied core section is recorded. This interval coincides with Preboreal warming. The high abundance of benthic ostracods may be linked to high nutrient input brought from deeper parts of the basin. A gradual reconnection of the Mediterranean with the Black Sea during this interval facilitated the entry of dense salty water in the deeper parts of the basin, thus pushing significant amounts of nutrients upslope. Boomer et al. (2010) identifies in core MD04-2754 (NW Black Sea shelf, 453 m water depth) a similar ostracod assemblage in the uppermost part of Unit 3 (Fig. 7). They gave a 14C age of this interval of high ostracod abundance at  $9390 \pm 80^{-14}$ C a bp (uncalibrated). Synchronously, anoxia became established in the deeper part of the Black Sea. At the top of this interval, in the Sapropel Mud, no in situ ostracod and foraminifera taxa are recorded.

### Ecological interval 1

The ostracod assemblages of this interval are dominated by marine Mediterranean taxa that adapted to salinities between 17 and 21% (Table 2). Ostracods of Caspian origin are almost completely replaced by Mediterranean ones. According to Zenina et al. (2017), Caspian ostracods dominate over Mediterranean ones until  $\sim$ 7100 cal a BP; thereafter, Mediterranean fauna become more abundant. Zenina et al. (2017) show that the transition from the first appearance of Mediterranean species ( $\sim$ 9600 cal a BP) to the disappearance of the last Caspian species ( $\sim$ 6800 cal a bp) took place at  $\sim$ 2800 cal a BP.

This interval contains a total of nine ostracod species, belonging to seven genera (Fig. 3). The sedimentation rate is very low, due to interrupted deposition at the shelf edge and a high-energy bottom water environment that led to mixture and washing away of sediments. This interval corresponds to Unit 1 and it is only 7 cm thick. The coccolith laminae contain blooms of the calcareous nannoplankton species *Emiliania huxleyi*. Foraminiferal taxa of the genus *Ammonia* show a very high abundance, typical for a brackish–marine environment with well- oxygenated waters (Briceag and Ion, 2014). Today, the bottom waters from this area, *i.e.* at 200 m water depth, are anoxic. The presence of the benthic ostracod and foraminiferal species argues for an oscillation of the anoxia base level since the Holocene through time.

### **Conclusions**

The integration of micropaleontological,  $\delta^{18}$ O, CaCO<sub>3</sub> and AMS <sup>14</sup>C data obtained from two studied cores (09 SG 13 and EuxRO\_2), located on the Romanian Black Sea outermost shelf, allow the identification of major changes in the Black Sea hydrology from the LGM to the Early Holocene interval. The radiocarbon dates from core 09 SG 13 cover an interval of 28 500 cal a BP.

Based on the abundance and diversity of ostracod assemblages, six ecological intervals were identified, corresponding to shifts in climate and salinity. To summarize, our main findings are:

- i. The LGM period was characterized by stable and cold climate mirrored by ostracod assemblages containing homogeneous fresh to slightly brackish taxa that prefer salinities up to 5–8‰
- ii. The very low salinity values (0.5–5‰) are linked to the first Meltwater Pulse during HS-1. This paleoenvironmental change is reflected in modifications to the ostracod assemblage, such as increased freshwater species diversity and abundance of the Loxoconchidae and Leptocytheridae. This bio-event reached a maximum during the Bølling–Allerød warm period, when Leptocytheridae dominate the ostracod assemblage. The δ¹8O drop related to the onset of the Meltwater Pulse is attributed to increased runoff into the Black Sea basin.
- iii. The Younger Dryas cold period is recorded in core 09 SG 13. The shift from a Loxoconchidae-dominated ostracod assemblage to Candonidae, at the top of the Younger Dryas, suggests a slight increase in salinity. During this cold interval the  $\delta^{18}$ O isotope values also display a slight increase. The Preboreal warming is mirrored in the ostracod assemblages by a significant increase in abundance.
- iv. Based on the coexistence of Ponto-Caspian and Mediterranean ostracods, the Late Holocene salinity of the NW Black Sea shelf area is estimated to be around 15‰.

Acknowledgements. We thank to the whole crew of the research vessel Mare Nigrum (owner GeoEcoMar), for support during the scientific cruises on the Black Sea. We are in debt to Prof. Dr Werner Piller, who kindly helped us to perform micropaleontological studies via SEM at Graz University. We are in debt to the late General Director of GeoEcoMar, Dr Gheorghe Oaie, who provided the studied cores, to Dr Irina Catianis for her assistance with measurements of organic matter and carbonate content and to the late geologist Constantin Ungureanu who helped us with sedimentological studies. The financial support for this paper was provided by the Romanian Ministry of Research and Innovation, through the Programme 1 -Development of the National System of Research - Institutional Performance, Project of Excellence in Research-Innovation, Contract No. 8PFE/2018 and by the Project uBiogas, contract no. 24PCCDI/ 2018. We acknowledge two anonymous reviewers and the Editor Prof. Geoffrey Duller for their constructive criticism that greatly helped to improve the quality of the paper.

Abbreviations. AMS, accelerator mass spectrometry; bsf, below the sea floor; HS-1, Heinrich Stadial 1; LGM, Last Glacial Maximum; MIS-2, marine isotope stage 2; OM, organic matter; SAR, sediment accumulation rate; YD, Younger Dryas.

#### References

- Aksu AE, Hiscott RN, Kaminski MA *et al.* 2002. Last Glacial—Holocene paleoceanography of the Black Sea and Marmara Sea: stable isotopic, foraminiferal and coccolith evidence. *Marine Geology* **190**: 119–149.
- Aksu AE, Hiscott RN, Yaşar D. 1999. Oscillating Quaternary water levels of the Marmara Sea and vigorous outflow into the Aegean Sea from the Marmara Sea–Black Sea drainage corridor. *Marine Geology* **153**: 275–302.
- Badertscher S, Fleitmann D, Cheng H *et al.* 2011. Pleistocene water intrusions from the Mediterranean and Caspian seas into the Black Sea. *Nature Geoscience* **4**: 236–239.
- Bahr A, Arz HW, Lamy F *et al.* 2006. Late glacial to Holocene paleoenvironmental evolution of the Black Sea, reconstructed with stable oxygen isotope records obtained on ostracod shells. *Earth and Planetary Science Letters* **241**: 863–875.
- Bahr A, Lamy F, Arz H *et al.* 2005. Late glacial to Holocene climate and sedimentation history in the NW Black Sea. *Marine Geology* **214**: 309–322
- Bahr A, Lamy F, Arz HW *et al.* 2008. Abrupt changes of temperature and water chemistry in the Late Pleistocene and Early Holocene Black Sea. *Geochemistry, Geophysics, Geosystems* **9**: DOI: 10.1029/2007GC001683.
- Balkas T, Dechev G, Mihnea R *et al.* 1990. State of the marine environment in the Black Sea Region. *UNEP Regional Seas Reports and Studies* **124**: 41.
- Bony G, Morhange C, Marriner N *et al.* 2015. History and influence of the Danube delta lobes on the evolution of the ancient harbour of Orgame (Dobrogea, Romania). *Journal of Archaeological Science* **61**: 186–203.
- Boomer I, Guichard F, Lericolais G. 2010. Late Pleistocene to Recent ostracod assemblages from the western Black Sea. *Journal of Micropalaeontology* **29**: 119–133.
- Boomer I, Horne DJ, Slipper IJ. 2003. The use of ostracods in palaeoenvironmental studies, or what can you do with an ostracod shell? *Paleontological Society Papers* **9**: 153–179.
- Briceag A, Ion G. 2014. Holocene ostracod and foraminiferal assemblages of the Romanian Black Sea shelf. *Quaternary International* **345**: 119–129.
- Briceag A, Stoica M, Oaie G *et al.* 2012. Late Holocene microfaunal and nannofloral assemblages of the NW Black Sea. *Geo-Eco-Marina* **18**: 65–73.
- Briceag A, Yanchilina A, Ryan WBF *et al.* 2016. Late Pleistocene—Holocene paleoenvironmental changes from the Romanian Black Sea shelf inferred by microfaunal and isotope fluctuations. *International Multidisciplinary Scientific Geoconference SGEM* 1: 305–312.
- Chepalyga AL. 1984. Inland sea basins. In *Late Quaternary Environments of the Soviet Union*, Velichkno AA (ed.). University of Minnesota Press: Minneapolis; 229–247.
- Chepalyga AL. 2007. The late glacial great flood in the Ponto-Caspian basin. In *The Black Sea Flood Question: Changes in Coastline,*

- Climate, and Human Settlement, Yanko-Hombach V, Gilbert AS, Panin N et al. (eds). Springer: Berlin; 119–148.
- Chepalyga AL, Sadchicova TA, Leonova NB et al. 2004. Caspian-Black Sea water exchange along Manych-Kerch Watergate in the Late Pleistocene. In Ekologiia antropogena i sovremennosti: priroda i chelovek" Sbornik statey Mezhdunarodnoi Konferentsii (Ecology of the Anthropogene and Contemporaneity: Nature and Man). Papers from the Int. Conf. (24–27 September 2004, Volgograd-Astrakhan), Humanistica: 50–53.
- Constantinescu AM, Toucanne S, Dennielou B *et al.* 2015. Evolution of the Danube deep-sea fan since the last glacial maximum: new insights into Black Sea water-level fluctuations. *Marine Geology* **367**: 50–68.
- Dinu C, Wong HK, Ţambrea D *et al.* 2005. Stratigraphic and structural characteristics of the Romanian Black Sea shelf. *Tectonophysics* **410**: 417–435.
- Fedorov PV. 1972. Postglacial transgression of the Black Sea. *International Geology Review* **14**: 160–164.
- Fleitmann D, Cheng H, Badertscher S *et al.* 2009. Timing and climatic impact of Greenland interstadials recorded in stalagmites from northern Turkey. *Geophysical Research Letters* **36**: 1–5.
- Georgiev YS. 1967. On dynamics of cold intermediate layer in the Black Sea. In *Okeanograficheskiye Issledovaniya Chernogo Morya* (*Oceanographic Investigations of the Black Sea*). Naukova Dumka, Kiev; 105–113.
- Goncharov VP. 1958. New data on the Black Sea bottom relief. *Dokl. Acad. Sc USSR* **121**: 830–833.
- Grosswald MG. 1980. Late Weichselian Ice Sheet of Northern Eurasia. *Quaternary Research* **13**: 1–32.
- Grosswald MG, Hughes TJ. 2002. The Russian component of an Arctic ice sheet during the Last Glacial Maximum. *Quaternary Science Reviews* **21**: 121–146.
- Gunnerson CG, Ozturgut E. 1974. The Bosphorus. In *The Black Sea: Geology, Chemistry, and Biology,* Degens ET, Ross DA (eds). American Association of Petroleum Geologists: Tulsa; 99–114.
- Hiscott RN, Aksu AE, Mudie PJ et al. 2007. The Marmara Sea Gateway since ~16 ky BP: non-catastrophic causes of paleoceanographic events in the Black Sea at 8.4 and 7.15 ky BP. In *The Black Sea Flood Question: Changes in Coastline, Climate, and Human Settlement,* Yanko-Hombach V, Gilbert AS, Panin N et al. (eds). Springer: Dordrecht; 89–117.
- Hiscott RN, Aksu AE, Yaşar D *et al.* 2002. Deltas south of the Bosphorus Strait record persistent Black Sea outflow to the Marmara Sea since ~10 ka. *Marine Geology* **190**: 95–118.
- Ivanova EV, Marret F, Zenina MA *et al.* 2015. The Holocene Black Sea reconnection to the Mediterranean Sea: new insights from the northeastern Caucasian shelf. *Palaeogeography, Palaeoclimatology, Palaeoecology* **427**: 41–61.
- Ivanova EV, Murdmaa IO, Chepalyga AL *et al.* 2007. Holocene sealevel oscillations and environmental changes on the eastern Black Sea shelf. *Palaeogeography, Palaeoclimatology, Palaeoecology* **246**: 228–259.
- Ivanova EV, Murdmaa IO, Karpuk MS *et al.* 2012. Paleoenvironmental changes on the northeastern and southwestern Black Sea shelves during the Holocene. *Quaternary International* **261**: 91–104.
- Kaminski MA, Aksu AE, Box M *et al.* 2002. Late Glacial to Holocene benthic foraminifera in the Marmara Sea: implications for Black Sea–Mediterranean Sea connections following the last deglaciation. *Marine Geology* **190**: 165–202.
- Khrischev KG, Georgiev VM. 1991. Regional washout on the Pleistocene–Holocene boundary in the western Black Sea Depression. *Comptes rendus de l'Académie bulgare des Sciences* **9**, Tome 44: 69–72.
- Konovalova VA. 2015. The species of the Family Ilyocyprididae Kaufmann, 1900 from the Pleistocene deposits of Western Siberia. *Modern micropaleontology: Proceedings of the XVI All-Russian Micropaleontological Meeting.* Kaliningrad; 85–88.
- Konovalova VA. 2016. Representatives of the genus Fabaeformiscandona Krstič, 1972 (Crustacea, Ostracoda) from Quaternary deposits of Western Siberia. *Revue de Micropaléontologie* **59**: 168–179.
- Kroonenberg SB, Rusakov GV, Svitoch AA. 1997. The wandering of the Volga Delta: a response to rapid Caspian sea-level change. *Sedimentary Geology* **107**: 189–209.
- Kwiecien O, Arz HW, Lamy F *et al.* 2008. Estimated reservoir ages of the Black Sea since the Last Glacial. *Radiocarbon* **50**: 99–118.

- Lericolais G, Bourget J, Popescu I et al. 2013. Late Quaternary deepsea sedimentation in the western Black Sea: new insights from recent coring and seismic data in the deep basin. Global and Planetary Change 103: 232–247.
- Lericolais G, Bulois C, Gillet H *et al.* 2009. High frequency sea level fluctuations recorded in the Black Sea since the LGM. *Global and Planetary Change* **66**: 65–75
- Lericolais G, Guichard F, Morigi C et al. 2010. A post Younger Dryas Black Sea regression identified from sequence stratigraphy correlated to core analysis and dating. Quaternary International 225: 199–209.
- Letouzey J, Biju-Dival B, Dorke A *et al.* 1977. The Black Sea: a marginal basin, geophysical and geological data. In *Structural History of the Mediterranean Basins*, Biju-Duval B, Montadert L (eds). Éditions Technip: Paris; 363–376.
- Major CO, Goldstein SL, Ryan WBF et al. 2006. The co-evolution of Black Sea level and composition through the last deglaciation and its paleoclimatic significance. Quaternary Science Reviews 25: 2031–2047.
- Major CO, Ryan WBF, Lericolais G *et al.* 2002. Constraints on Black Sea outflow to the Sea of Marmara during the last glacial—interglacial transition. *Marine Geology* **190**: 19–34.
- Margvelashvily N, Maderich V, Zheleznyak M. 1999. Simulation of radionuclide fluxes from the Dnieper-Bug Estuary into the Black Sea. *Journal of Environmental Radioactivity* **43**: 157–171.
- Marret F, Mudie PJ, Aksu AE *et al.* 2009. A Holocene dinocyst record of a two-step transformation of the Neoeuxinian brackish water lake into the Black Sea. *Quaternary International* **197**: 72–86.
- Meisch C. 2000. Freshwater Ostracoda of Western and Central Europe. Spektrum Academischer: Heidelberg.
- Mertens KN, Bradley LR, Takano Y *et al.* 2012. Quantitative estimation of Holocene surface salinity variation in the Black Sea using dinoflagellate cyst process length. *Quaternary Science Reviews* **39**: 45–59.
- Mudie PJ, Marret F, Aksu AE *et al.* 2007. Palynological evidence for climate change, anthropogenic activity and outflow of Black Sea water during the Late Pleistocene and Holocene: centennial- to decadal- scale records from the Black and Marmara Seas. *Quaternary International* **167–168**: 73–90.
- Nikishin AM, Ziegler PA, Panov DI et al. 2001. Mesozoic and Cainozoic evolution of the Scythian Platform–Black Sea–Caucasus domain. In *Peri-Tethyan Rift/Wrench Basins and Passive Margins*, Ziegler HK, Cavazza W, Robertson AF et al. (eds), *Peri-Tethys Memoir* 6: Mem. Mus. Natl. Hist. Nat.: Paris; 295–346.
- Oaie G, Melinte-Dobrinescu MC. 2012. Holocene litho- and biostratigraphy of the NW Black Sea (Romanian shelf). *Quaternary International* **261**: 146–155.
- Olteanu R. 1978. Ostracoda from DSDP Leg 42B. *Initial Reports of the Deep-Sea Drilling Project* 42: 1017–1038.
- Opreanu PA. 2006. Studiul populațiilor de ostracode actuale și fosile de pe platforma continentală a Mării Negre. Universitatea "Ovidius" Constanta, *PhD Thesis*, 273 p.
- Opreanu PA. 2008. Ostracode relicte Ponto-Caspice in sectorul Românesc al Mării Negre. *GeoEcoMarina* **14**: 57–62.
- Özsoy E, Latif MA, Tuğrul S *et al.* 1995. Exchanges with the Mediterranean, fluxes and boundary mixing processes in the Black Sea. In *Mediterranean Tributary Seas*, Briand F (ed.). Bulletin Institute Océanographie Monaco, Special No. 15, CIESM Science Series 1: 1–25
- Panin N, Jipa D. 2002. Danube River Sediment Input and its Interaction with the North-western Black Sea. *Estuarine, Coastal and Shelf Science* **54**: 551–562.
- Piper DZ, Calvert SE. 2009. A marine biogeochemical perspective on black shale deposition. *Earth-Science Reviews* **95**: 63–96.
- Piper DZ, Calvert SE. 2011. Holocene and late glacial palaeoceanography and palaeolimnology of the Black Sea: changing sediment provenance and basin hydrography over the past 20,000 years. *Geochimica et Cosmochimica Acta* **75**: 5597–5624.
- Popescu I, Lericolais G, Panin N *et al.* 2001. Late Quaternary channel avulsions on the Danube Deep-Sea Fan, Black Sea. *Marine Geology* **179**: 25–37.
- Qin B, Yu G. 1998. Implications of lake level variations at 6 ka and 18 ka in mainland Asia. *Global and Planetary Change* **18**: 59–72.
- Reimer PJ, Bard E, Bayliss A et al. 2013. IntCal13 and Marine13 radiocarbon age calibration curves 0–50,000 years cal BP. Radiocarbon 55: 1869–1887.

- Ross DA, Degens ET. 1974. Recent sediments of the Black Sea. In *The Black Sea: Geology, Chemistry, and Biology,* Degens ET, Ross DA (eds). American Association of Petroleum Geologists: Tulsa; 183–199.
- Ryan WBF. 2007. Status of the Black Sea flood hypothesis. In *The Black Sea Flood Question: Changes in Coastline, Climate, and Human Settlement,* Yanko-Hombach V, Gilbert AS, Panin N *et al.* (eds). Springer: Berlin; 63–88.
- Ryan WBF, Major CO, Lericolais G et al. 2003. Catastrophic flooding of the Black Sea. *Annual Review of Earth and Planetary Sciences* **31**: 525–554.
- Ryan WBF, Pitman WC, Major CO *et al.* 1997. An abrupt drowning of the Black Sea shelf. *Marine Geology* **138**: 119–126.
- Ryan WBF, Yanchilina A, Matamoros E et al. 2013. Massive meltwater discharge into the Black Sea Euxine Lake. *Proceedings of the 14th RCMNS Congress*; 87.
- Schornikov El. 1964. An experiment on the distinction of the Caspian elements of the ostracod fauna in the Azov-Black Sea basin. *Zoologicheski Zurnal* **43**: 1276–1293.
- Schornikov El. 2011. Ostracoda of the Caspian origin in the Azov-Black Sea basin. In *European Ostracodologists Meeting, Abstract Volume,* Gross M (ed.). Universalmuseum Joanneum: Graz; 180–184.
- Shumilovskikh LS, Tarasov P, Arz HW *et al.* 2012. Vegetation and environmental dynamics in the southern Black Sea region since 18 kyr bp derived from the marine core 22-GC3. *Palaeogeography, Palaeoclimatology, Palaeoecology* **337–338**: 177–193.
- Soulet G, Ménot G, Bayon G et al. 2013. Abrupt drainage cycles of the Fennoscandian Ice Sheet. *Proceedings of the National Academy of Sciences* **110**: 6682–6687.
- Soulet G, Ménot G, Garreta V et al. 2011a. Black Sea 'Lake' reservoir age evolution since the Last Glacial hydrologic and climatic implications. Earth and Planetary Science Letters 308: 245–258.
- Soulet G, Ménot G, Lericolais G *et al.* 2011b. A revised calendar age for the last reconnection of the Black Sea to the global ocean. *Quaternary Science Reviews* **30**: 1019–1026.
- Stancheva M. 1989. Taxonomy and biostratigraphy of the Pleistocene ostracods of the western Black Sea Shelf. *Geologica Balcanica* 19: 3–39.
- Tolmazin D. 1985. Changing coastal oceanography of the Black Sea. I: Northwestern shelf. *Progress in Oceanography* **15**: 217–276.
- Wegwerth A, Kaiser J, Dellwig O *et al.* 2016. Northern hemisphere climate control on the environmental dynamics in the glacial Black Sea 'Lake'. *Quaternary Science Reviews* **135**: 41–53.
- Williams LR, Hiscott RN, Aksu AE *et al.* 2018. Holocene paleoecology and paleoceanography of the southwestern Black Sea shelf revealed by ostracod assemblages. *Marine Micropaleontology* **142**: 48–66.
- Yanchilina AG, Ryan WBF, McManus JF *et al.* 2017. Compilation of geophysical, geochronological, and geochemical evidence indicates a rapid Mediterranean-derived submergence of the Black Sea's shelf and subsequent substantial salinification in the Early Holocene. *Marine Geology* **383**: 14–34.
- Yanchilina AG, Ryan WBF, McManus JF et al. 2018. Reply to comment on: "Compilation of geophysical, geochronological, and geochemical evidence indicates a rapid Mediterranean-derived submergence of the Black Sea's shelf and subsequent substantial salinification in the early Holocene" by Yanchilina AG, Ryan WBF, McManus JF et al. [Marine Geology 383 (2017) 14-34]. Marine Geology 407: 354–361.
- Yanko VV. 1990. Stratigraphy and paleogeography of marine Pleistocene and Holocene deposits of the southern seas of the USSR. *Memorie della Società Geologica Italiana* **44**: 167–187.
- Yanko-Hombach V. 2007. Controversy over Noah's Flood in the Black Sea: geological and foraminiferal evidence from the shelf. In *The Black Sea Flood Question: Changes in Coastline, Climate, and Human Settlement,* Yanko-Hombach V, Gilbert AS, Panin N *et al.* (eds). Springer: Berlin; 149–203.
- Yanko-Hombach V, Kondariuk T, Motnenko I. 2017. Benthic foraminifera indicate environmental stress from river discharge to marine ecosystems: example from the Black Sea. *Journal of Foraminiferal Research* **47**: 70–92.
- Zenina MA, Ivanova EV, Bradley LR *et al.* 2017. Origin, migration pathways, and paleoenvironmental significance of Holocene ostracod records from the northeastern Black Sea shelf. *Quaternary Research* 87: 49–65.